CONVECTION CELLS IN THE ATMOSPHERIC BOUNDARY LAYER

Katherine Fodor and Juan Pedro Mellado

Max Planck Institute for Meteorology, Bundesstr. 53, 20146 Hamburg

MOTIVATION

Turbulent convection self-organises on large scales into circulation cells; an example of coherent structures in turbulence.

Open cellular convection over the Gulf of Mexico on 2. November 2014. Image from NASA Worldview.

Previous work on coherent structures in the atmospheric boundary layer (ABL) has helped to establish their existence, persistence and importance to transport between the surface and the free atmosphere [1-4]. Yet there is still uncertainty regarding the behaviour of these large-scale circulations (LSCs), their dependence on boundary conditions and how they affect small-scale properties. We aim to reduce these uncertainties.

RESEARCH QUESTIONS

The open cells observed in the convective boundary layer (CBL) bear a stark resemblance to those observed in other free convective regimes such as Rayleigh-Bénard convection [5].

We exploit this apparent similarity to gain a deeper understanding of what controls large-scale organisation in free convection, aiming to answer the following questions:

Q1 How can we appropriately and efficiently extract LSCs from the flow field in each case?

Q2 Do observed similarities between LSCs in different free convective regimes translate to statistical similarities? Do LSCs have properties which are universal to all free convective regimes?

Q3 How can we express the differences in LSC properties between configurations in terms of the boundary conditions and controlling parameters?

As a result of this work, we will obtain insight into the dynamics of LSCs not only in the CBL, but for free convection as a whole. Ultimately we aim to study the interaction between LSCs and small-scale turbulence. In this poster we mainly address Q1.

METHOD

We perform direct numerical simulation (DNS) of the Boussinesq equations in two-dimensions for four different cases of free convection (described below). We investigate the efficacy of various techniques for detecting LSCs, including time averaging, spatial filtering and proper orthogonal decomposition (POD):

- **Spatial Filtering:** We use a box (or top-hat) filter of width Δ.
- **Temporal Filtering:** We average over an interval of length T. We also consider shifting fields horizontally every $\Delta t \ll T$ to maximise the correlation with the field at the previous time [6].
- **POD:** We use the same time interval length, T, as used in the time averaging so as to compare methods.

Here we use the following parameters in all cases:

- Prandtl number, $Pr = \nu/\kappa = 1$.
- Free-fall Reynolds number, $Re_f = \left(H^3\Delta b\right)^{\frac{1}{2}}/\nu = O(10^4)$,
  Free-fall Rayleigh number, $Ra_f = Re_f^2 Pr = \left(H^3\Delta b\right)/(\nu\kappa) = O(10^8)$.
- Aspect ratio, $\Gamma = 5.6$.

Δb is the vertical buoyancy difference across the convection cell.

FOUR CASES: LARGE-SCALE CIRCULATION DETECTION

Rayleigh-Bénard convection (RBC):

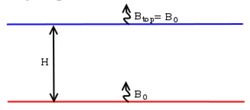

Control parameters:
$\{B_0, \nu, \kappa, H\}$
steady, non-penetrative

RBC with adiabatic top lid (LID):

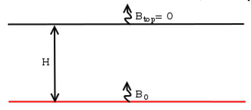

Control parameters:
$\{B_0, \nu, \kappa, H\}$
quasi-steady, non-penetrative

CBL growing into stably-stratified layer (qCBL):

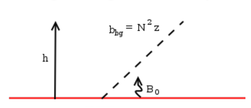

Control parameters:
$\{B_0, \nu, \kappa, N\}$
quasi-steady, penetrative

CBL growing into non-stratified layer (uCBL):

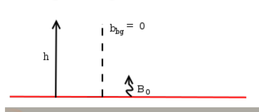

Control parameters:
$\{B_0, \nu, \kappa\}$
unsteady, penetrative

Snapshot of the buoyancy field:
Red is positively buoyant fluid, blue is negatively buoyant fluid.

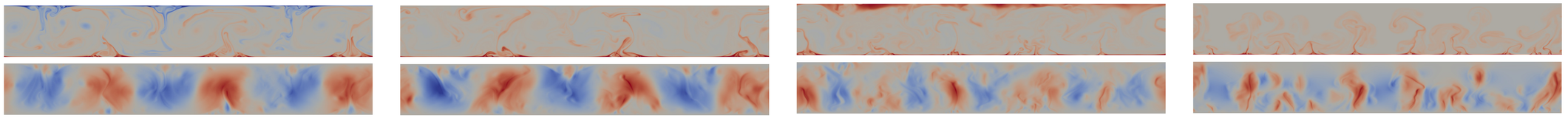

Snapshot of the vertical velocity field:
Red is rising fluid, blue is sinking fluid.

Spatially filtered vertical velocity field:

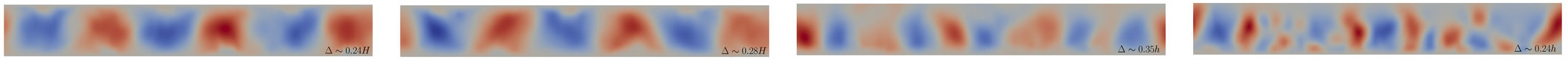

Temporally filtered vertical velocity field:

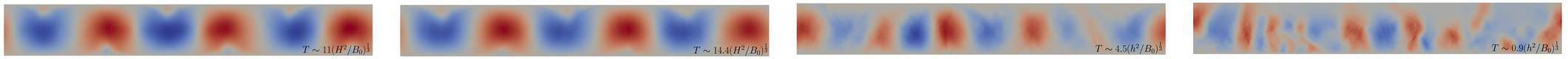

First POD mode of the vertical velocity field:

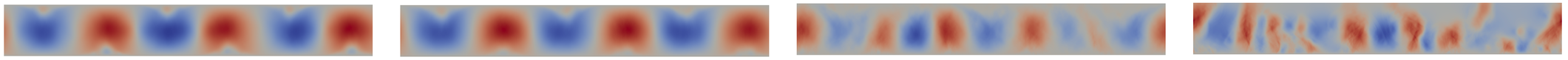

CONCLUSIONS

Spatial Filtering:

- The vertically integrated turbulent kinetic energy (TKE) at first decreases linearly with filter width in all cases, demonstrating the sensitivity to the choice of filter width.
- The decrease is at least twice as fast in penetrative cases, highlighting that the CBL contains more smaller scales of motion than RBC due to entrainment.
- However, LSCs are not defined exclusively by their size, but also by their longevity.

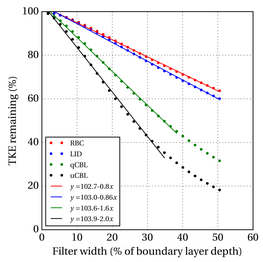

Temporal Filtering:

- In the CBL, both the number and location of LSCs change in time, whereas in RBC they remain fixed.
- Shifting fields horizontally to maximise the correlation with the previous time eliminates the effect of fields decorrelating due only to their translation, but decreases the mean decorrelation time, suggesting this scenario does not occur often.
- A running average over the mean decorrelation time results in a stronger signal that is more representative of LSCs as they change in time.

	RBC	LID	qCBL	uCBL
TKE remaining [%]	83%	78%	51%	53%
Corresponding spatial filter width, Δ	$\sim 0.24H$	$\sim 0.28H$	$\sim 0.33h$	$\sim 0.24h$

Vertically integrated TKE remaining after temporal filtering and the spatial filter width, Δ, required to obtain the same decrease in TKE.

Proper Orthogonal Decomposition:

- Similarly to temporal filtering, the results depend on the time interval, T, used.
- Restricting the time interval to be the same as that used in the temporal filtering yields almost identical results.

Main Conclusion:

Since the computational cost of POD is much greater than temporal or spatial filtering, the latter seem to be more effective methods for extracting LSCs in all cases.

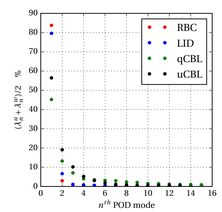

TKE contained in each POD mode as a percentage of the sum over all modes.

[1] H. Schmidt and U. Schumann (1989), 'Coherent structure of the convective boundary layer derived from large-eddy simulations', *J. Fluid Mech.* **200**, 511–562.

[2] De Roode et al. (2004), 'Large-Eddy Simulation: How Large is Large Enough?', *J. Atm. Sci.* **61**, 403–421.

[3] A. Hellsten and S. Zilitinkevich (2013), 'Role of Convective Structures and Background Turbulence in the Dry Convective Boundary Layer', *Boundary-Layer Meteorol.* **149**, 323–353.

[4] J. P. Mellado et al. (2016), 'Near-Surface Effects of Free Atmosphere Stratification in Free Convection', *Boundary-Layer Meteorol.* **159**, 69–95.

[5] M. S. Emran and J. Schumacher (2015), 'Large-scale mean patterns in turbulent convection', *J. Fluid Mech.* **776**, 96–108.

[6] M. van Reeuwijk et al. (2008), 'Wind and boundary layers in Rayleigh-Bénard convection. I. Analysis and Modeling', *Physical Review E.* **77**, 036311.

Max-Planck-Institut für Meteorologie

IMPRS-ESM International Max Planck Research School on Earth System Modelling

DFG Turbulent Superstructures